ADVANCED MATERIALS

over timescales of hundreds of seconds ($0.00\ \mu m^2 s^{-1}$). It is interesting that in the neutral MEA experiment, in which some of the surface amine groups are protonated, the diffusion coefficient was slightly lower than in the other cases.

A surprising result was obtained when measuring the diffusion coefficients of the three sizes of MESA particles on the neutral surface derivatized with hexadecanethiol ($C_{16}H_{33}SH$). Comparing *D* values to those found on the MESA surface, we found near agreement for all but the small-diameter particles ($6\ \mu m \times 90$ nm), which reproducibly stuck to the substrate immediately on contact. For larger particles, the long-range electrostatic force (presumably between the negatively charged sulfonate groups and an image charge in the substrate) is expected to dominate,[22] but for smaller ones the short-range van der Waals force is more important. Apparently, the two are closely balanced for the $C_{16}H_{33}SH$ functionalized surface with rods of the size investigated here.

While the scaling of these interactions is not completely understood at present, these initial studies provide some guidance as to the conditions that are desirable for nanorod assembly experiments. The observation of pH-dependent diffusion may, for example, be useful for affixing particles to specific areas or in specific conformations on basic surfaces. More importantly, the particle tracking method described here provides a simple and convenient method for quantifying the surface diffusion of non-spherical particles under arbitrary conditions.

Experimental

Whatman Al_2O_3 filter membranes that contain 300–350 nm diameter internal pores were used as a template material. For 90 nm internal pore diameter, Al_2O_3 membranes were prepared in-house by the electrochemical anodization of an Al plate [23]. In both cases, one face of the membranes was coated with approximately 150 nm of thermally evaporated Ag. More Ag was electrodeposited (Silver 1024, Technic, Inc.) directly onto the evaporated Ag in order to close any open pores. This Ag layer was then used as the back contact in the electrochemical cell, and more Ag was deposited, further filling-in the pores. The membrane and cell were rinsed with deionized H_2O, and Au solution was added (Orotemp, Technic, Inc.). Plating was stopped with the desired rod length was reached. The Ag backing was removed by dissolving in 2 mL of 50 % HNO_3, and the Al_2O_3 template was dissolved in 2 mL of 5 M NaOH. The rods were sedimented using a laboratory centrifuge. The supernatant was removed and water was added. The rods were resuspended by physical agitation and brief immersion in an ultrasonic water bath. This rinsing process was repeated a total of five times in order to prepare the rods for addition of self-assembled monolayers (SAMs). Rods were derivatized with 2-mercaptoethanesulfonic acid, sodium salt (MESA, Aldrich) by suspending them in 1 mL of 1 mM MESA(aq) for 1 h. The MESA rods were then rinsed as described above, suspended in a total volume of 1 mL, and diluted 1000-fold for imaging.

Microscope slides coated with 5 nm Cr/100 nm Au (EMF) were used as derivatizable surfaces in these experiments. Prior to derivatization, surfaces were cleaned with piranha solution (3:1 conc. H_2SO_4/30 % H_2O_2). After copious rinsing with water, the Au-coated slides were placed in 10 mM MESA(aq), 2-mercaptoethylamine (MEA, Aldrich) (aq), or hexadecanethiol (Avocado Research Chemicals, Ltd.) (ethanol) for 1 h. The slides were rinsed with water, in the cases of MESA and MEA, or ethanol, in the case of hexadecanethiol. The surfaces were then dried under a stream of Ar. MEA slides were further treated with acidic or basic solutions in order to effect the protonation of the amino groups. Each MEA surface was rinsed with 0.01 M HCl(aq), 0.01 M NaOH(aq), or water, and immediately dried under Ar. The solutions were of pH 2.9, pH 12.6, and pH 8.5, respectively.

Received: October 9, 2002

[1] Z. Adamczyk, P. Warszynski, L. Szyk-Warszynska, P. Weronski, *Colloids Surf. A* **2000**, *165*, 157.
[2] M. S. Hale, J. G. Mitchell, *Nano Lett.* **2001**, *1*, 617.
[3] *Solid/Liquid Dispersions* (Ed: T. F. Tardos), Academic Press, Bracknell **1987**.
[4] W. R. Bowen, A. Mongruel, *Colloids Surf. A* **1998**, *138*, 161.
[5] C. A. Murray, D. G. Grier, *Annu. Rev. Phys. Chem.* **1996**, *47*, 421.
[6] J. A. Weiss, D. W. Oxtoby, D. G. Grier, C. A. Murray, *J. Chem. Phys.* **1995**, *103*, 1180.
[7] D. G. Grier, C. A. Murray, *J. Chem. Phys.* **1994**, *100*, 9088.
[8] D. G. Grier, C. A. Murray, in *Ordering and Phase Transitions in Charged Colloids* (Eds: A. K. Arora, B. V. R. Tata), Wiley-VCH, Weinheim **1996**, pp. 69–100.
[9] Z. Dogic, S. Fraden, *Phys. Rev. Lett.* **1997**, *78*, 2417.
[10] P. A. Smith, C. D. Nordquist, T. N. Jackson, T. S. Mayer, B. R. Martin, J. K. N. Mbindyo, T. E. Mallouk, *Appl. Phys. Lett.* **2000**, *77*, 1399.
[11] J. K. N. Mbindyo, B. D. Reiss, B. R. Martin, C. D. Keating, M. J. Natan, T. E. Mallouk, *Adv. Mater.* **2001**, *13*, 249.
[12] Y. Huang, X. F. Duan, Q. Q. Wei, C. M. Lieber, *Science* **2001**, *292*, 702.
[13] D. Spisak, *Phys. A* **1994**, *209*, 42.
[14] J. Parkinson, K. E. Kadler, A. Brass, *Phys. Rev. E* **1994**, *50*, 2963.
[15] F. de J. Guevara-Rodriguez, M. Medina-Noyola, *Phys. Rev. E* **2000**, *61*, 6368.
[16] J. M. Lahtinen, T. Hjelt, T. Ala-Nissila, Z. Chvoj, *Phys. Rev. E* **2001**, *64*, 21 204.
[17] A. Vincze, L. Demko, M. Vörös, M. Zrínyi, M. N. Esmail, Z. Hórvölgyi, *J. Phys. Chem. B* **2002**, *106*, 2404.
[18] M. Takeo, *Disperse Systems*, Wiley-VCH, Weinhein **1999**, pp. 43–60.
[19] B. R. Martin, D. J. Dermody, B. D. Reiss, M. Fang, L. A. Lyon, M. J. Natan, T. E. Mallouk, *Adv. Mater.* **1999**, *11*, 1021.
[20] B. R. Martin, S. K. St. Angelo, T. E. Mallouk, *Adv. Funct. Mater.* **2002**, *12*, 759.
[21] L. P. Faucheux, A. J. Libchaber, *Phys. Rev. E* **1994**, *49*, 5158.
[22] S. Ross, I. D. Morrison, *Colloidal Systems and Interfaces*, John Wiley & Sons, New York **1988**, pp. 205–210.
[23] K. Nielsch, F. Müller, A. Li, U. Gösele, *Adv. Mater.* **2000**, *12*, 582.

Morphogenesis of One-Dimensional ZnO Nano- and Microcrystals**

By *Haoquan Yan*, *Rongrui He*, *Johnny Pham*, and *Peidong Yang**

During the past few years, much effort has been invested in controlling the sizes and shapes of inorganic nanocrystals, because these parameters represent key elements that determine their electrical and optical properties.[1,2] One way to achieve shape control is to enhance anisotropic nanocrystal growth using a liquid medium. The vapor–liquid–solid (VLS) growth mechanism, in which the nanowires grow out of supersaturated liquid alloy droplets, has been extremely successful in creating one-dimensional nanomaterials.[3–5] Another common approach is to use surfactants, regular or inverse micelles

[*] Prof. P. Yang, H. Yan, R. He, J. Pham
Department of Chemistry, Lawrence Berkeley National Laboratory
University of California at Berkeley
Berkeley, CA 94720 (USA)
E-mail: p_yang@uclink.berkeley.edu

[**] This work was supported by the Camille and Henry Dreyfus Foundation, 3M Corporation, Beckman Foundation, Research Corporation, and the National Science Foundation. P.Y. is an Alfred P. Sloan Research Fellow. Work at the Lawrence Berkeley National Laboratory was supported by the Office of Science, Basic Energy Sciences, Division of Materials Science of the US Department of Energy. We thank the National Center for Electron Microscopy for the use of their facilities.

  0935-9648/03/0503-0402 $ 17.50+.50/0

as regulating agents, or templates to facilitate anisotropic crystal growth.[6,7] This method has been used extensively in synthesizing many inorganic nanocrystals, nanorods, and nanowires, e.g., CdSe,[8] Au,[9] Co,[10] $BaWO_4$,[11] $[Mo_3Se_3]^-$.[12] Nanocrystals of tetrapods, teardrops, and arrows have been successfully synthesized by carefully controlling the nucleation and growth within a solution medium.[13]

More recently, the vapor process has been explored to produce one-dimensional nanostructures of different cross sections as well as some other exotic shapes.[4] We report here our deterministic growth of different shapes of ZnO crystals from the nanometer to the micrometer scale. Simple evaporation and condensation of different zinc vapor sources in oxygen was explored. Tetrapods and dendrites have been synthesized by simply adjusting the reaction temperature and the partial pressure of oxygen within the system. Size control of the tetrapods and one-dimensional nanowire arrays can be achieved by varying the growth time and the ratio between zinc vapor pressure and oxygen partial pressure. In addition, ZnO nanoribbons can be synthesized by carbon-thermal reduction of ZnO powders at relatively low temperature.

During our systematic exploration of the zinc oxide nanowire synthetic process,[14–16] we discovered a simple approach to synthesize different morphologies of ZnO nano- and microcrystals. The chemical vapor transport and condensation (CVTC) process used the gas phase reaction between Zn vapor and O_2 to grow ZnO crystals. Shape control was achieved by carefully tuning the ratio of the oxygen partial pressure and the Zn vapor pressure. At constant flow of oxygen and argon mixture (0.5–5 % O_2 in argon, with flow rate of 10 sccm), uniform tetrapods with hexagonal cylindrical arms were synthesized with large yield (> 95 %). When the oxygen partial pressure was larger than 5 % during the growth process, tetrapods with trumpet-like arms were formed.

Figure 1 shows typical scanning electron microscopy (SEM) images of the ZnO tetrapods. The diameter of the arms can be tuned from 100 nm to 2 μm by increasing the oxygen partial pressure from 0.5 % to 5 %. The thin tetrapods generally have needle-shaped arms (Fig. 1a), while the thick ones have uniform hexagonal cylinder arms (Fig. 1b,c). X-ray diffraction recorded on these tetrapods can be readily indexed according to the wurtzite ZnO crystal structure.

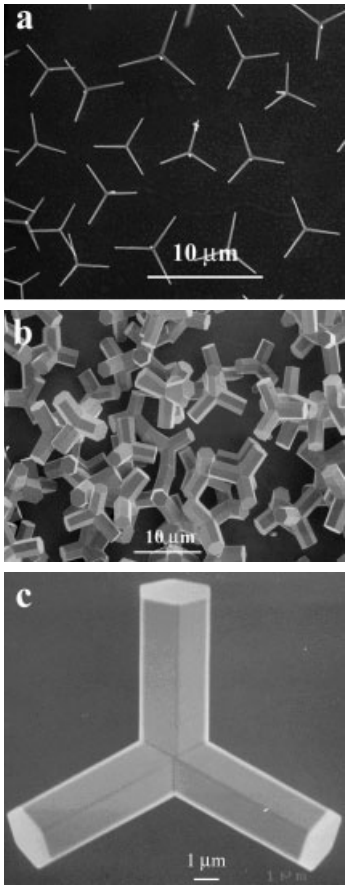

Fig. 1. SEM images of ZnO tetrapods with different diameters. a) ZnO tetrapods with arms of 200 nm diameter. b) ZnO tetrapods with arms of 2 μm diameter. c) High-magnification SEM image of a single ZnO tetrapod with an arm of 2 μm diameter.

Selected area diffraction (SAD) on the arms of the tetrapods shows that all four arms are single-crystalline and grow along the <001> direction. Detailed transmission electron microscopy (TEM) studies on a tripod (a tetrapod with one arm missing) provide more structural information, see Figure 2. The tripod in Figure 2a was tilted to the [201] zone axis of arm I and the corresponding SAD pattern is shown in the inset in Figure 2b. As shown in Figure 2b, the dark field image based on the $(10\bar{2})$ reflection spot on arm I shows that arm I

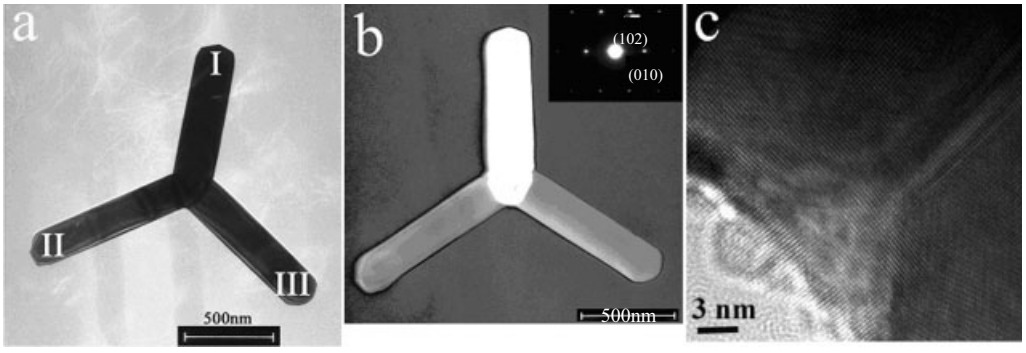

Fig. 2. a) TEM image of a tripod. b) Dark field image of arm I recorded on the $[10\bar{2}]$ spot along the [201] zone axis. The inset is the SAD pattern of arm I of the tripod. c) High-resolution TEM image at the joint of the tripod.

  0935-9648/03/0503-0403 $ 17.50+.50/0

ADVANCED MATERIALS

extends all the way through the center of the tripod. A high-resolution TEM image at the joint of the tripod (Fig. 2c) shows the interface between two nanowire arms, where the boundary between the arm and core with the same wurtzite structure can be readily seen. These observations are quite different from the zinc-blend core structure that Kitano et al. have proposed.[17] It is also quite different from nanocrystalline CdSe tetrapod formation, where zinc-blende CdSe was found in the core.[13] The existence of a wurtzite nanocrystal core, however, is consistent with early scanning electron microscopy studies carried out by Iwanaga and co-workers.[18–20]

Two types of ZnO tetrapods (Figs. 1 and 3) can be synthesized by controlling the oxygen partial pressure during the growth process. Figure 1c shows typical tetrapods with hexagonal cylinder arms. These tetrapods are grown under low oxygen partial pressure (0.5–5 %). When we increase the oxygen partial pressure to 5–10 %, tetrapods with trumpet-like arms were formed at high yield (Fig. 3). The exact reason for this subtle change in morphology is not clear at this stage, but it is

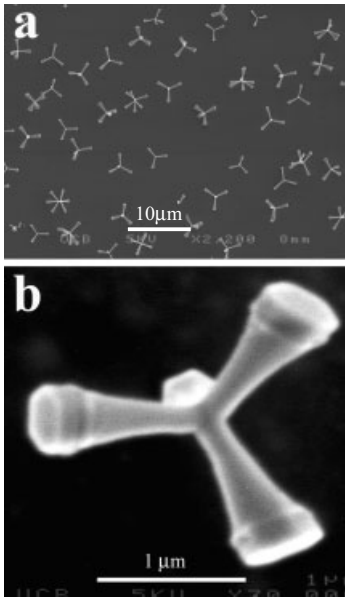

Fig. 3. SEM images of ZnO tetrapods with trumpet-like arms at low (a) and high (b) magnification.

most likely linked to dynamic crystal growth processes at different oxygen partial pressure. At low oxygen partial pressure, ZnO crystal growth is slow. It approximately undergoes a thermodynamical equilibrium during the growth process, which would result in regular-shaped hexagonal cylinder arms. At high oxygen partial pressure, the growth of ZnO crystals might be kinetically controlled, since the growth rates of the <001> and <100> directions depend on the oxygen partial pressure to a different extent. As a result, trumpet-shaped arms would form.

Interestingly, these uniform ZnO tetrapods could be used as building blocks for a self-assembly study. Figure 4 shows self-assembly of these tetrapod units into dimers (Fig. 4b,c) and tetramers (inset in Fig. 4a). These ZnO tetrapod "oligomers"

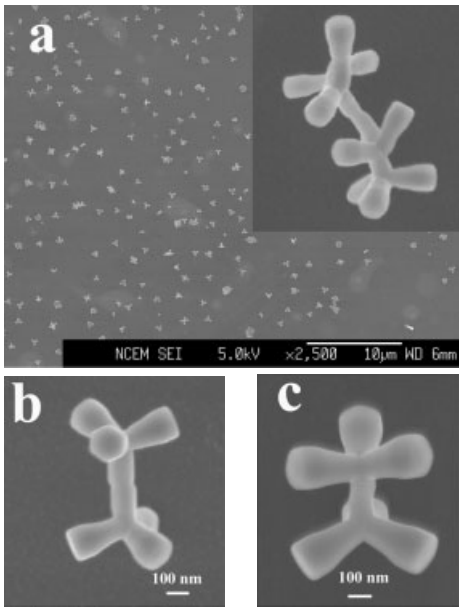

Fig. 4. SEM images of self-assembled ZnO tetrapods. a) A low-magnification SEM image of ZnO tetrapods with trumpet-shaped arms. The inset image is a tetramer formed from the ZnO tetrapods. b) Staggered form of the ZnO tetrapod dimer. c) Eclipsed form of the ZnO tetrapod dimer.

are quite similar to alkanes, where the tetrapods resemble four-coordinated carbon atoms. They can even form different space configurations. Figures 4b and 4c show two different dimers with a "staggered" and an "eclipsed" configuration, respectively, resembling those of the ethane molecules.

In addition, we found that a high yield of microscale comb-like structures made of periodic arrays of single-crystalline ZnO nanowires can be produced when the substrate is placed right next to the Zn evaporation source. Figure 5a shows a typical SEM image of these ZnO nanowire comb structures.

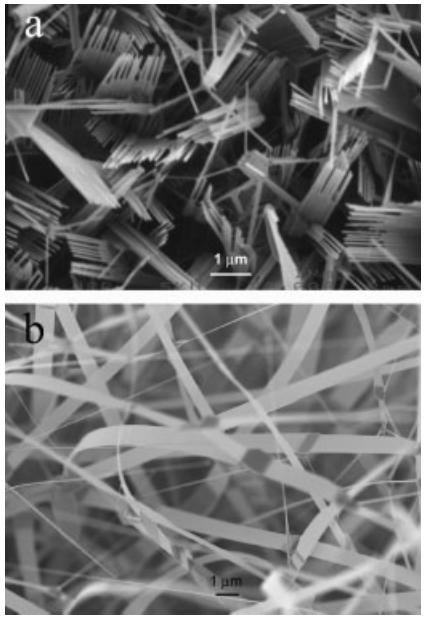

Fig. 5. a). SEM image of comb structures made of ZnO nanowires. b) SEM image of ZnO nanoribbons synthesized at 900 °C.

  0935-9648/03/0503-0404 $ 17.50+.50/0

The nanowire branches have uniform diameters and are evenly distributed at one or both sides of the stem. The diameters of the nanowires range from 20 to 120 nm and their lengths are 2–10 μm. X-ray diffraction (XRD) confirms the wurtzite structure of the entire microfern structures. Additional TEM structural characterization indicates that these hierarchically ordered nanowire arrays are single crystalline and monolithic.

When a ZnO and carbon mixture was used as the Zn vapor source, ZnO crystals with different morphologies were also observed. Noticeably, when the ZnO/C (1:1) mixture was heated up to 900 °C in a similar growth system, a high yield (> 95 %) of ZnO nanoribbons are produced after the reaction. Normally the length of the ribbons is about 20–60 μm, the width is about 1 μm, and the thickness is about 100–200 nm (Fig. 5b). TEM characterization indicates that most of the ZnO nanoribbons adopted a similar structure to the one reported by Wang and co-workers:[21] they grow along the $[01\bar{1}0]$ direction and are enclosed by $\pm(2\bar{1}\bar{1}0)$ and ±(0001) facets. Importantly, compared with the high-temperature evaporation and condensation method (1400 °C for ZnO nanoribbons) that Wang and co-workers used, our growth temperature is much lower (900 °C). This indicates that such a very high temperature is not necessary for nanoribbon nucleation and growth. Currently, the exact growth mechanism of these ribbon-shaped nanostructures is still under investigation.

Our deterministic growth of different shapes of ZnO crystals from the nanometer to micrometer scale offers ideal model systems to study the optical properties within different microcavities.[14–16,22,23] These nano- and microcrystals can be further used as building blocks to assemble two- or three-dimensional assemblies.[24]

Experimental

ZnO tetrapods and dendrites were synthesized using a chemical vapor transport and condensation system developed in our lab. Zn powder (Alfa Aesar, 99.999 %) was used as Zn source. The source material was placed in an alumina boat located in the center of a quartz tube in a tube furnace. The substrates were placed downstream of the carrier gas flow. As carrier gas a 5–10 % O_2/Ar mixture was used, with a flow rate of 8–10 sccm. The reaction was carried out at 800–900 °C and kept at that temperature for 10–30 min. After the reaction, the substrate was coated with a thin layer of white powder.

ZnO nanoribbons were synthesized in the same manner by using a 1:1 ZnO/C mixture as Zn vapor source. The substrates were coated with 20 Å Au and they were put on top of the alumina boat, located at the center of a quartz tube in the tube furnace. Pure argon was constantly flowed at about 10 sccm as the carrier gas. The reaction was carried out at 900 °C for 10 min.

The crystal structures were analyzed using XRD (Siemens D5000). The morphology and size distribution of the crystals were characterized using SEM (JOEL 6400 or JSM-6430 operated at 5 keV). TEM studies of the crystals were carried out on a Philips CM200 operated at 200 keV.

Received: October 9, 2002

[1] C. M. Lieber, *Solid State Commun.* **1998**, *107*, 607.
[2] A. P. Alivisatos, *Science* **1996**, *271*, 933.
[3] J. T. Hu, T. W. Odom, C. M. Lieber, *Acc. Chem. Res.* **1999**, *32*, 435.
[4] P. Yang, Y. Wu, R. Fan, *Int. J. Nanosci.* **2002**, *1*, 1.
[5] Y. Wu, P. Yang, *J. Am. Chem. Soc.* **2001**, *123*, 3165.
[6] M. Li, H. Schnablegger, S. Mann, *Nature* **1999**, *402*, 393.
[7] J. Tanori, M. P. Pileni, *Langmuir* **1997**, *13*, 639.
[8] Z. A. Peng, X. G. Peng, *J. Am. Chem. Soc.* **2002**, *124*, 3343.
[9] Y. Y. Yu, S. S. Chang, C. L. Lee, C. R. C. Wang, *J. Phys. Chem. B* **1997**, *101*, 6661.
[10] V. F. Puntes, K. M. Krishnan, A. P. Alivisatos, *Science* **2001**, *291*, 2115.
[11] S. Kwan, F. Kim, J. Arkana, P. Yang, *Chem. Commun.* **2001**, 447.
[12] B. Messer, J. H. Song, M. Huang, Y. Wu, F. Kim, P. Yang, *Adv. Mater.* **2000**, *12*, 1526.
[13] L. Manna, E. C. Scher, A. P. Alivisatos, *J. Am. Chem. Soc.* **2000**, *122*, 12 700.
[14] M. Huang, S. Mao, H. Feick, H. Yan, Y. Wu, H. Kind, E. Weber, R. Russo, P. Yang, *Science* **2001**, *292*, 1897.
[15] J. Johnson, H. Yan, R. Schaller, L. Haber, R. Saykally, P. Yang, *J. Phys. Chem. B* **2001**, *105*, 11 387.
[16] P. Yang, H. Yan, S. Mao, R. Russo, J. Justin, R. Saykally, N. Morris, J. Pham, R. He, H. Choi, *Adv. Funct. Mater.* **2002**, *12*, 323.
[17] M. Kitano, T. Hamabe, S. Maeda, T. Okabe, *J. Cryst. Growth* **1993**, *128*, 1099.
[18] M. Fujii, H. Iwanaga, M. Ichihara, S. Takeuchi, *J. Cryst. Growth* **1993**, *128*, 1095.
[19] H. Iwanaga, M. Fujii, S. Takeuchi, *J. Cryst. Growth* **1993**, *134*, 275.
[20] H. Iwanaga, M. Fujii, M. Ichihara, S. Takeuchi, *J. Cryst. Growth* **1994**, *141*, 234.
[21] Z. Pan, Z. Dai, Z. Wang, *Science* **2001**, *291*, 1947.
[22] J. O. Vasseur, P. A. Deymire, L. Dobrzynski, B. Djafari-Rouhani, A. Akjouj, *Phys. Rev. B* **1997**, *55*, 10 434.
[23] W. Nakagawa, R. Tyan, P. Sun, Y. Fainman, *Opt. Express* **2000**, *7*, 123.
[24] T. D. Clark, J. Tien, D. C. Duffy, K. E. Paul, G. M. Whitesides, *J. Am. Chem. Soc.* **2001**, *123*, 7677.

Formation of Silver Nanowires Through a Sandwiched Reduction Process**

By *Yujie Xiong*, *Yi Xie*,* *Changzheng Wu*, *Jun Yang*, *Zhengquan Li*, and *Fen Xu*

Controlling the shape of nanostructures at the mesoscopic level is one of the most challenging issues presently faced by synthetic chemists. Especially in the past few years, metal nanowires, which are one-dimensional (1D) objects, have attracted particular interest, due to their unusual roles in the fabrication of nanoscale electronic devices and investigation of quantized conductance and localization effects.[1–5] Silver, as the metal with the highest electrical and thermal conductivity, has many significant applications, and thus the preparation of its nanowires has received the most attention.

How can atoms or other building blocks be relationally assembled into structures with nanoscale diameter but much longer lengths, thus forming a 1D nanostructure? Many methods have been developed to prepare silver nanowires, for example electrochemical techniques[6–8] or in emulsion or polymeric systems.[9–14] Some templates, such as mesoporous

[*] Prof. Y. Xie, Dr. Y. Xiong
Structure Research Laboratory, Department of Chemistry
University of Science and Technology of China
Hefei, Anhui 230026 (People's Republic of China)
E-mail: yxielab@ustc.edu.cn
Dr. C. Wu, J. Yang, Dr. Z. Li, Dr. F. Xu
Department of Chemistry
University of Science and Technology of China
Hefei, Anhui 230026 (People's Republic of China)

[**] This work was supported by the Chinese National Natural Science Foundation and the Foundation for the Authors of Nationally Excellent Doctoral Dissertations of P. R. China (Project No. 199923).

  0935-9648/03/0503-0405 $ 17.50+.50/0